

# The Effect of Pulse Phase Errors on the Chirp Scaling SAR Processing Algorithm

Gordon W. Davidson, *Member, IEEE*, Frank Wong, *Member, IEEE*, and Ian Cumming, *Member, IEEE*

**Abstract**—The chirp scaling (CS) SAR processing algorithm uses the linear FM property of the transmitted pulses to provide accurate range cell migration correction. However, when the transmitted pulse is not linear FM, or if the FM rate is not known exactly, processing errors due to chirp scaling will result. This paper presents the resulting processing error in the CS algorithm, given pulse phase errors that exceed those expected in current SAR systems. The registration and phase error that result in chirp scaling are negligible for typical or stable pulse phase errors, or can be avoided if phase modulation coefficients are estimated from the replica. A fast Fourier transformed pulse replica is sufficient to form the range matched filter in the CS algorithm, giving slightly better range resolution than the range/Doppler (R/D) algorithm.

## I. INTRODUCTION

IN image formation from synthetic aperture radar (SAR) data, the range cell migration correction (RCMC) processing step is a range-dependent signal shift that is required to compensate for the varying distance from the sensor to a point scatterer. The range/Doppler (R/D) algorithm [1] uses an interpolator for this step in the range time and azimuth frequency domain, which must be truncated at the expense of accuracy. Chirp scaling (CS) is a new algorithm which uses the linear FM property of the received, uncompressed pulses to remove the range dependence of RCMC. Then the bulk RCMC is performed in the two-dimensional frequency domain [2], thus avoiding the issue of interpolator truncation.

However, chirp scaling assumes a linear FM pulse of a known frequency rate, so that phase modulation errors in the transmitted pulse may affect the accuracy of CS processing. It is well known that pulse phase errors, if not accounted for during pulse compression, lead to range resolution broadening and increased sidelobe level [3]. Aside from this effect on pulse compression, pulse phase errors have no further effect on the R/D algorithm.

In this paper, Section II presents the model for a SAR signal which includes a general pulse phase error, and the resulting processing error due to chirp scaling is described in the two-dimensional frequency domain in Section III. Also, the use of a pulse replica to obtain the pulse compression filter is dis-

cussed, since this may be affected by chirp scaling. Section IV presents the effects on chirp scaling of quadratic, cubic, and cyclic pulse phase errors. Simulations verify the calculated processing errors, and compare the results of processing with chirp scaling in the presence of phase errors, with the results of the R/D algorithm.

## II. SIGNAL MODEL

Assume that the nominal transmitted pulse is linear FM of frequency rate  $K$ . The deviation of the actual pulse from this specification is modeled as a phase error  $\varepsilon(\tau)$ , where  $\tau$  is range time, giving the transmitted pulse

$$p(\tau) = m(\tau) \exp\{-j\pi K\tau^2 - j2\pi\varepsilon(\tau)\} \quad (1)$$

where  $m(\tau)$  is the amplitude of the pulse. The phase error is assumed to be much smaller than the total pulse phase.

Pulse compression can be represented in the frequency domain as a multiplication by the conjugate of the Fourier transform of the pulse. It is shown in the Appendix that to first order, the spectrum of the pulse with a general phase error can be expressed as

$$P(f_\tau) = M(f_\tau) \exp\left\{\frac{j\pi f_\tau^2}{K} - j2\pi\varepsilon\left(\frac{-f_\tau}{K}\right)\right\} \quad (2)$$

where  $f_\tau$  is range frequency and  $M(f_\tau)$  is the amplitude spectrum. If pulse compression is performed assuming the nominal transmitted pulse, then the compression error is represented in the frequency domain by the unmatched phase term  $-2\pi\varepsilon(f_\tau/K)$ .

SAR data consists of the backscattered returns of pulses transmitted while the sensor is at different azimuth (along track) positions. Both the CS and R/D algorithms perform certain processing steps in the range time/azimuth frequency (or R/D) domain, which is obtained by taking an azimuth fast Fourier transform of the data. Consider the SAR data received from a single point scatterer at closest approach range,  $r$ , and the corresponding SAR signal in the R/D domain. In this domain, the SAR signal without pulse phase errors consists of linear FM signals in the range time direction, at each azimuth frequency,  $f_\eta$ . Including the pulse phase error, the R/D signal can be shown to be

$$S(f_\eta, \tau; r) = H_a(f_\eta; r) m\left(\frac{K_m}{K}(\tau - \tau_d)\right) \exp\left[-j\pi K_m(\tau - \tau_d)^2 - j2\pi\varepsilon\left(\frac{K_m}{K}(\tau - \tau_d)\right)\right] \quad (3)$$

Manuscript received January 24, 1995; revised June 27, 1995. This work was supported by the B.C. Science Council, the NSERC, the B.C. Advanced Systems Institute, and MacDonald Dettwiler.

G. W. Davidson was with the Department of Electrical Engineering, University of British Columbia, Vancouver, B.C. V6T 1Z4 Canada. He is now with German Aerospace Research Establishment, 82234 Oberpfaffenhofen, Germany.

F. Wong is with MacDonald Dettwiler, Richmond, B.C. V6V 2J3 Canada. I. Cumming is with the Department of Electrical Engineering, University of British Columbia, Vancouver, B.C. V6T 1Z4 Canada.

Publisher Item Identifier S 0196-2892(96)01002-9.

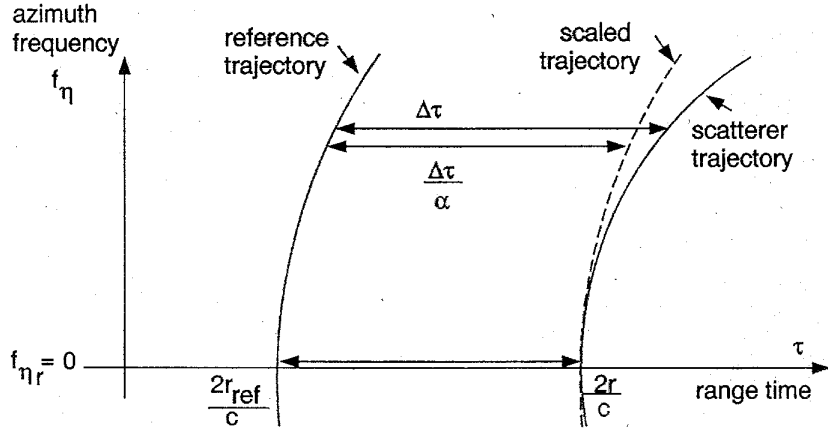


Fig. 1. Signal trajectories and effect of chirp scaling.

where  $H_a(f_\eta; r)$  represents the azimuth phase variation for azimuth compression. The frequency rate of each signal in the range direction is described by  $K_m(f_\eta; r)$ , where the modification from  $K$  is accommodated by secondary range compression (SRC) [2]. Also, the phase center of each signal is delayed in range time, at each azimuth frequency, by an amount  $\tau_d(f_\eta; r)$ . This azimuth frequency dependent delay defines a nearly hyperbolic trajectory of signal energy in the R/D domain. The trajectory shape depends on the closest approach range of the scatterer, and the purpose of RCMC is to straighten the trajectories for scatterers at all ranges.

### III. ERRORS IN CHIRP SCALING

In order to implement range variant RCMC in the chirp scaling algorithm, each uncompressed range line in the R/D signal is multiplied by a chirp scaling phase function. The phase function is centered on a reference trajectory corresponding to a reference range,  $r_{\text{ref}}$ , which is typically at midswath. Within a range line for a given azimuth frequency, this phase function multiply changes the phase structure of each uncompressed pulse, so that a range-dependent shift is achieved in the location of each pulse after compression, as shown in Fig. 1. At a given azimuth frequency,  $f_\eta$ , the shift for the scatterer at  $r$  depends on the range time difference of the trajectory from the reference trajectory,  $\Delta\tau(f_\eta; r) = \tau_d(f_\eta; r) - \tau_d(f_\eta; r_{\text{ref}})$ . This range-dependent shift can be considered as a scaling of the range-time axis at each azimuth frequency, by a scale factor,  $\alpha(f_\eta)$ . For a given scatterer trajectory, the effect of the shifts at different azimuth frequencies is to change the trajectory to the scaled trajectory, shown in Fig. 1, which has the same shape as the reference trajectory. Thus the scaled trajectories for scatterers at all ranges have the same shape. After the phase function multiply in the R/D domain, a Fourier transform in the range direction takes the data to the two-dimensional frequency domain, where the bulk range-invariant RCMC is performed by adding a linear phase term to the range compression and SRC filters, as described in [2].

#### A. Pulse Errors

However, the processing assumes linear FM pulses without phase modulation errors. By applying the steps of the chirp

scaling algorithm to a SAR signal which includes pulse phase errors, a phase term in the two-dimensional frequency domain arises which depends upon  $\epsilon$ , and thus is not accounted for during processing. This phase error term is given by

$$\phi_\epsilon(f_\eta, f_\tau; r) = -2\pi\epsilon \left[ \frac{-f_\tau - K_m(f_\eta; r)[\alpha(f_\eta) - 1]\Delta\tau(f_\eta; r)}{\alpha(f_\eta)K} \right]. \quad (4)$$

A phase error in the frequency domain such as  $\phi_\epsilon(f_\eta, f_\tau; r)$  results in image degradation such as impulse response broadening and registration errors [4]. If no chirp scaling is applied, corresponding to the case of  $\alpha = 1$ , then  $\phi_\epsilon(f_\eta, f_\tau; r)$  reduces to the phase error in the pulse spectrum in (2) and thus represents the error in pulse compression. With chirp scaling, the difference between (4) and the pulse compression error represents the additional processing errors introduced by the interaction of pulse phase errors with chirp scaling:

$$\Delta\phi_\epsilon(f_\eta, f_\tau; r) = -2\pi \left\{ \epsilon \left[ \frac{-f_\tau - K_m(f_\eta; r)[\alpha(f_\eta) - 1]\Delta\tau(f_\eta; r)}{\alpha(f_\eta)K} \right] - \epsilon \left[ \frac{-f_\tau}{K} \right] \right\}. \quad (5)$$

In general,  $\alpha(f_\eta)$  is close to unity, and  $\Delta\tau(f_\eta; r)$  is related to range difference of a scatterer from the reference range. Thus, the azimuth frequency and range dependence of the processing phase error in (5) is determined mostly by the term

$$[\alpha(f_\eta) - 1]\Delta\tau(f_\eta; r) \quad (6)$$

which is proportional to the amount of shift of the trajectory for a scatterer at range  $r$ . In this term,  $[\alpha(f_\eta) - 1]$  is an indication of the amount of scaling, and as seen in Fig. 1, this depends on the azimuth frequency difference from the reference azimuth frequency,  $f_{\eta r}$ , where the scatterer trajectory and scaled trajectory intersect [2]. Fig. 1 illustrates the case for  $f_{\eta r} = 0$ , which is useful for relatively small squint angles since it results in scatterers in the processed image being registered at closest approach range. In this case, the scale factor,  $\alpha(f_\eta)$ , is approximately  $[1/\cos(\theta_\eta)]$ , where  $\theta_\eta$

is the azimuth look direction within the antenna beam that corresponds to the azimuth frequency,  $f_\eta$ .

Since the processing phase error in (4) depends on azimuth frequency, the possibility exists of a coupling of pulse errors into processing errors in the azimuth direction, in the form of an azimuth registration error and azimuth impulse response broadening. However, the processing phase error was calculated as a function of azimuth frequency, using the spaceborne SAR parameters discussed in the results below. It was found in all cases that the total change in phase error across the azimuth frequency band was less than  $8^\circ$ , which is negligible. Also, the change in RCMC error across the azimuth frequency band, given in the results below is very small. Thus, the effect of pulse phase errors on azimuth focussing can be neglected, and a one dimensional analysis in the range direction is sufficient. Because of the very small variation of processing error across the azimuth frequency band, the effect of the scale factor,  $\alpha(f_\eta)$ , on processing error can be described as a function of the squint angle,  $\theta$ , to beam center. In the results presented below, a squint angle of  $5^\circ$  is used, with  $f_{\eta r} = 0$  to give a worst case amount of scaling for conventional SAR.

Finally, if a replica of the transmitted pulse in (1) is available, then it can be used to improve the accuracy of range compression. The replica can be fast Fourier transformed to get the pulse spectrum,  $P(f_\tau)$ , and the range matched filter is then obtained by multiplying  $P(f_\tau)$  by phase factors to accommodate SRC and the change in range frequency rate caused by chirp scaling [2]. The information about the pulse phase modulation error in this case is through the presence in the replica of the phase error term, as described in (2), so the remaining processing error is the additional error due to chirp scaling in (5). An effect of using the fast Fourier transformed replica is that the magnitude of  $P(f_\tau)$  is included in the range matched filter. In chirp scaling, the multiplication of the signal by the phase function introduces a range-dependent range frequency shift in the signal:

$$\delta f_\tau = -[\alpha(f_\eta) - 1]K_m(f_\eta; r)\Delta\tau(f_\eta; r). \quad (7)$$

Thus, when the range matched filter multiply is applied in the range frequency domain, some frequency components of the signal are shifted outside of the interval spanned by the magnitude of  $P(f_\tau)$ . The result is a small loss of range bandwidth. The frequency shift itself is later removed by the phase correction step in chirp scaling in the R/D domain [2].

Alternatively, phase modulation coefficients can be estimated from the replica. In this case, an accurate value of frequency rate can be used in chirp scaling. A cubic phase modulation error, even if known, may still result in a processing error because of the deviation from the linear FM assumption in chirp scaling. Also, with this use of the replica, the range matched filter can be calculated from the phase modulation coefficients, and an appropriate magnitude weighting chosen so as to avoid the loss of range bandwidth to the frequency shift in chirp scaling.

### B. Range-Dependence Errors

While the main source of errors considered in this paper is the phase error in the transmitted pulse, there exists a

similar error that is inherent in the R/D signal. This is the range dependence of the frequency rate,  $K_m(f_\eta; r)$ , of the linear FM signals in the range Doppler domain. In the chirp scaling algorithm, the scaling and range compression (including SRC) is performed at each azimuth frequency, so the  $f_\eta$  dependence of  $K_m(f_\eta; r)$  is accommodated. However, the algorithm assumes a range-invariant frequency rate in SRC and in the chirp scaling phase function, where the frequency rate is determined at a reference range,  $r_{\text{ref}}$  [2]. Thus, for a scatterer at range,  $r$ , a frequency rate error is introduced in the R/D domain. From (3) it can be seen that this can be represented by the equivalent pulse phase error

$$\varepsilon(\tau) = [K_m(f_\eta; r) - K_m(f_\eta; r_{\text{ref}})] \frac{K^2}{K_m^2(f_\eta; r)} \tau^2 \quad (8)$$

with the same effects on range compression and chirp scaling as a frequency rate error in the transmitted pulse.

However, for the spaceborne SAR parameters and the  $5^\circ$  squint angle considered in the results below, the range dependence of  $K_m(f_\eta; r)$  is quite small. For L-band, the maximum quadratic phase error for a scatterer at the swath edge is about  $12^\circ$ , and for C-band it is about  $3^\circ$ . This is too small to affect chirp scaling, as will be seen in the results. In range compression, the effect on resolution width is negligible, and since the variation of  $K_m$  is known, any phase error in the compressed pulse can be compensated by a complex multiply. For higher squint angles, the range dependence of  $K_m(f_\eta; r)$  can affect range compression and chirp scaling, and in this case the extended chirp scaling algorithm presented in [5] may be used.

## IV. RESULTS

In this section, quadratic, cubic, and cyclic pulse phase errors are considered in the calculation and simulation of processing errors, since these are adequate to represent the transmitted pulse phase for most sensors [6]. Pulse phase errors that exceed those expected in SAR systems are investigated, in order to get worst case results.

For quadratic and cubic pulse phase errors, the resulting processing error in (4) is calculated, where the processing error is expressed as a sum of phase terms in powers of range frequency,  $f_\tau$ , where the terms correspond to errors in pulse compression, RCMC, and phase of the compressed pulse. The calculations use L-band and C-band spaceborne SAR parameters, with a squint angle of  $5^\circ$  and  $f_{\eta r} = 0$ . Some processing errors are range dependent, being zero at the reference range and increasing toward the edge of the swath. Thus the scatterer is assumed to be at the swath edge, 20 km in slant range from the reference range. In addition, at the swath edge the maximum range frequency shift due to chirp scaling in each case is less than 1.7% of the range bandwidth.

The simulations are used to verify the calculations and to compare the processing results of the CS and R/D algorithms for quadratic, cubic, and cyclic pulse phase errors. In the simulations, only L-band parameters are used since the processing errors are slightly larger than for C-band. The signal received from a point scatterer is simulated with a rectangular weighted

pulse, and the range signal is assumed to be oversampled by 15%. The simulated signal is processed with the CS and R/D algorithms, where in the R/D algorithm an eight-point interpolator is used in RCMC. Also, the SRC filter is calculated accurately for both algorithms, so that this comparison of the CS and R/D algorithms does not reflect the difference in SRC between the algorithms (i.e., the accommodation of azimuth frequency dependent SRC in the CS algorithm). The simulation results for quadratic, cubic, and cyclic phase errors are shown in Figs. 2 to 4, respectively, which show the magnitude plots of the range compressed pulse at the edge of the azimuth frequency band, processed with the CS (solid line) and R/D (dashed line) algorithms. The resulting compressed pulse in range is used to measure: the 3-dB resolution width in samples, registration error in samples, maximum sidelobe level, or integrated sidelobe ratio (ISLR) in decibels, and the phase error in degrees at the peak of the compressed pulse.

#### A. Quadratic Phase Error

An error in frequency rate,  $\Delta K$ , results in a quadratic pulse phase error that is modeled by

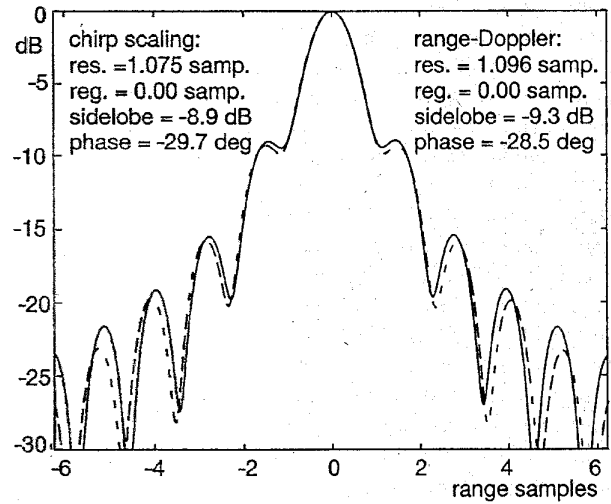
$$\varepsilon(\tau) = \frac{\Delta K \tau^2}{2}. \quad (9)$$

The total processing phase error in the two-dimensional frequency domain is evaluated using (4):

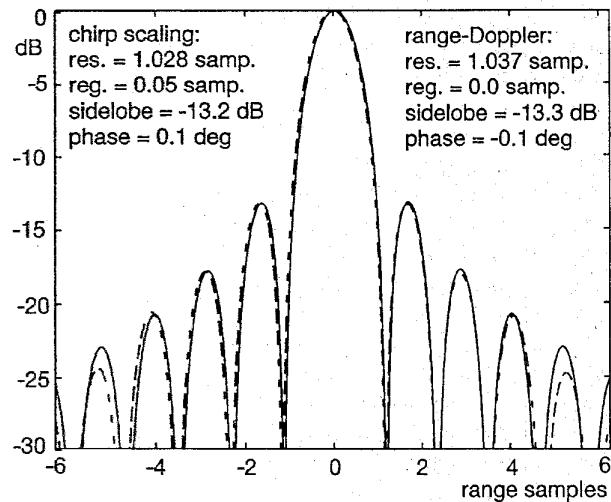
$$\phi_\varepsilon = -\frac{\pi \Delta K}{\alpha^2 K^2} f_\tau^2 - \frac{2\pi \Delta K K_m}{\alpha^2 K^2} (\alpha - 1) \Delta \tau f_\tau - \frac{\pi \Delta K K_m^2}{\alpha^2 K^2} (\alpha - 1)^2 \Delta \tau^2. \quad (10)$$

The processing errors were investigated for a frequency rate error in the transmitted pulse which would give a maximum quadratic phase error, in the absence of chirp scaling, of  $90^\circ$ . The range compression error term in (10) (the first term) is very close to the pulse spectrum phase error in the absence of chirp scaling: a difference in maximum quadratic phase error of about one degree. Thus the fast Fourier transformed pulse replica can effectively remove the range compression error. The maximum RCMC shift error (the second term) varies across the azimuth frequency band by 0.01 range samples for L-band, and 0.002 samples for C-band, and thus has a negligible effect on focussing. The RCMC shift error at the Doppler centroid gives the range-dependent registration error, which for each case is less than 0.04 samples at the swath edge. Finally, the constant phase error (the third term) is very small, being less than  $0.2^\circ$ .

The simulation results for this case are shown in Fig. 2, where results are given for the cases of a) no replica is used in pulse compression and b) a fast Fourier transformed replica is used to obtain the compression filter. When the pulse replica is fast Fourier transformed to obtain the range matched filter, the compression error is removed in both algorithms. Also, in this case the registration error in chirp scaling is just measurable, being about 0.05 samples at the swath edge. There is a slightly better resolution with the CS algorithm, because it does not suffer the bandwidth loss due to the interpolator in the R/D algorithm, for the given range oversampling rate and



(a)



(b)

Fig. 2. Magnitude of compressed range pulses processed with the chirp scaling (solid line) and R/D (dashed line) algorithms. Transmitted pulse had a quadratic phase error: (a) no replica; (b) fast Fourier transformed replica used to obtain matched filter.

interpolator length. On the other hand, with the CS algorithm some bandwidth is lost because of the frequency shift in chirp scaling. However, considering both these effects, the results in Fig. 2 show a slightly better resolution for the CS algorithm than for the R/D algorithm.

#### B. Cubic Phase Error

Next, consider a small deviation from linear FM in the transmitted pulse, represented by a cubic phase term

$$\varepsilon(\tau) = \frac{\Delta C \tau^3}{3}. \quad (11)$$

Evaluating  $\phi_\varepsilon(f_\eta, f_\tau; r)$  with this pulse phase error gives the processing phase error in the two-dimensional frequency

domain as

$$\begin{aligned} \phi_\varepsilon(f_\eta, f_\tau; r) = & \frac{2\pi\Delta C}{3\alpha^3 K^3} f_\tau^3 + \frac{2\pi\Delta CK_m}{\alpha^3 K^3} (\alpha - 1) \Delta\tau f_\tau^2 \\ & + \frac{2\pi\Delta CK_m^2}{\alpha^3 K^3} (\alpha - 1)^2 \Delta\tau^2 f_\tau \\ & + \frac{2\pi\Delta CK_m^3}{3\alpha^3 K^3} (\alpha - 1)^3 \Delta\tau^3. \end{aligned} \quad (12)$$

These processing errors were evaluated for a value of  $\Delta C$  which gives a maximum cubic phase error in the transmitted pulse of  $90^\circ$ . The cubic range compression term (the first term in (12)) differs from the pulse spectrum phase error in (2) by a maximum of  $1.5^\circ$ , so a fast Fourier transformed replica can be used to perform range compression. The quadratic term (the second term) is range dependent, and evaluated at the swath edge it gives a maximum quadratic phase error of  $11^\circ$  for L-band or C-band. This is too small to affect focussing but results in range dependent phase error in the peak of the range compressed pulse. The RCMC shift error (the third term) varies across the azimuth frequency band by less than 0.001 samples for L-band, and less than 0.0003 samples for C-band, and the registration error at the swath edge in each case is 0.002 samples, which is negligible. Finally, the constant phase error (the last term) is very small.

The simulation results are shown in Fig. 3, and results are given for the cases of: a) no replica; b) a fast Fourier transformed replica; and c) the matched filter calculated from phase coefficients known from simulation of the pulse (as if the accurate coefficients had been estimated from the replica). Comparing Fig. 3(a) and (b), it is seen that using a fast Fourier transformed replica to obtain the range matched filter successfully removes the compression error that results from the cubic phase error in the transmitted pulse. The registration error due to chirp scaling is too small to be measured, and the CS algorithm gives a slight improvement in resolution over the R/D algorithm. The resolution with chirp scaling improves further when the range matched filter is calculated using coefficients obtained from the replica, since in this case the loss of bandwidth due to the frequency shift in chirp scaling is avoided. The CS algorithm has a phase error in the compressed pulse of about  $3^\circ$  at the swath edge, which is due to the range dependent quadratic phase compression error resulting from the interaction of chirp scaling with the cubic pulse phase. If phase coefficients are estimated from the replica, this phase can be determined and removed by a complex multiply.

### C. Cyclic Phase Error

The effect of a cyclic pulse phase error on processing with chirp scaling can be deduced from the form of (4). Note that  $\phi_\varepsilon(f_\eta, f_\tau; r)$  is a shifted version of the pulse spectrum error,  $-2\pi\varepsilon(-f_\tau/K)$ , as a function of  $f_\tau$ . For a cyclic pulse phase error, such a shift does not change the nature of the processing error, compared to the pulse compression error, or introduce other types of image degradations. Thus, chirp scaling should not have a noticeable affect on processing with this type of pulse phase error.

To investigate a cyclic phase error, a pulse was simulated with a phase error:

$$\varepsilon(\tau) = \Delta Y \sin(\omega\tau) \quad (13)$$

where  $\omega$  was chosen to give ten cycles over the length of the pulse, and  $\Delta Y$  was chosen to give a relatively large peak phase error of  $15^\circ$ . The results of are shown in Fig. 4, for the cases of no replica and the use of a fast Fourier transformed replica. From the result with no replica it can be seen that the pulse phase error itself does not affect the performance of the CS algorithm compared to the R/D algorithm, although the results are slightly different because of the interpolator used in the R/D algorithm. The use of a replica does not remove the echoes in either algorithm, and this is because of the effect of the pulse phase error on the amplitude spectrum, which is not remedied by matched filtering. However, when the replica is used, there is a noticeable difference between the algorithms in the form of the echos of the compressed pulse, and the CS algorithm has a higher value of ISLR. This is due to the shifting of the signal phase spectrum by chirp scaling which causes a mismatch with the phase of the fast Fourier transformed replica. Thus, with chirp scaling, some phase error remains after compression which leads to a slightly higher echo, although for typical cyclical phase errors this effect should be small.

## V. DISCUSSION

### A. Processing Errors in Chirp Scaling

From the results presented above, the worst case effect of a maximum  $90^\circ$  quadratic pulse phase error on chirp scaling is a registration error that reaches about 0.05 range samples by the edge of the swath. The effect of maximum  $90^\circ$  cubic pulse phase error on chirp scaling is a range dependent, maximum  $11^\circ$  quadratic phase error, which is too small to affect resolution but results in a  $3^\circ$  compressed pulse phase error at the swath edge. The highest order phase error term in the range matched filter is not significantly affected by chirp scaling, so that a fast Fourier transformed pulse replica can be used in range compression.

For the pulse phase errors and SAR parameters considered here, these registration and phase errors are too small to affect the quality of the magnitude image, but may be noticeable in SAR interferometry. In interferometry, the phases of two images of the same scene are compared in order to infer terrain height, and accurate registration and phase of the images is essential [7]. However, if the transmitted pulse is stable between images, then the processing errors are consistent between the images and do not affect interferometric processing. Finally, the registration and phase error can be avoided if phase modulation coefficients are estimated from the pulse replica. In this case, the frequency rate is known accurately so the registration error due to a quadratic pulse phase error is avoided, and the compressed pulse phase error due to the cubic pulse phase error can be determined and removed by a complex multiply.

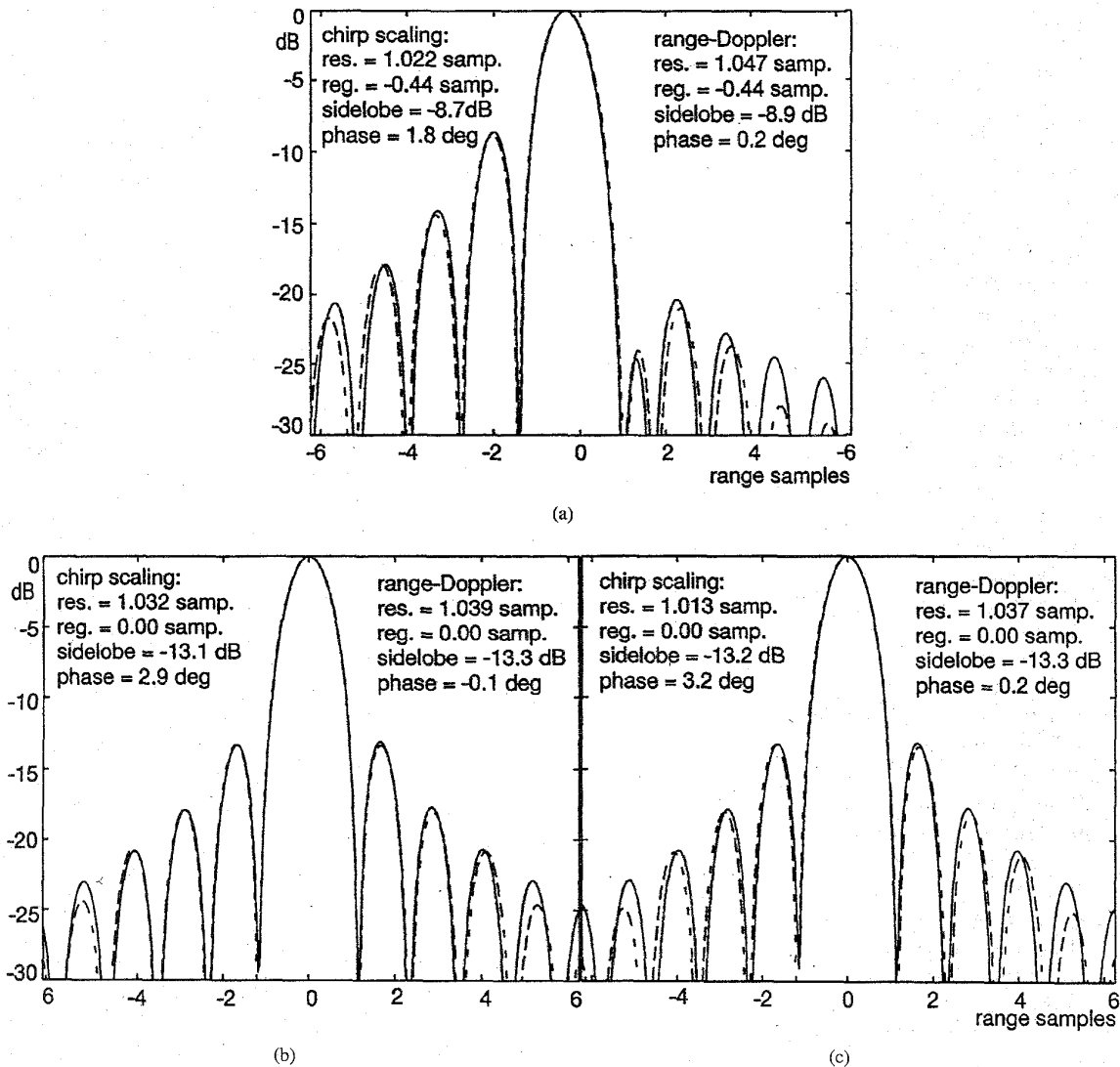


Fig. 3. Magnitude of compressed range pulses processed with the chirp scaling (solid line) and R/D (dashed line) algorithms. Transmitted pulse had a cubic phase error: (a) no replica; (b) fast Fourier transformed replica used to obtain matched filter; (c) matched filter calculated from phase coefficients obtained from replica.

### B. Chirp Scaling Sensitivity

Results of calculations and simulations are given above for particular values of pulse phase error, squint, reference azimuth frequency, and distance from the reference range. However, from (9) to (13), the general sensitivity of the CS algorithm to pulse phase errors and SAR parameters can be inferred.

The noticeable processing errors due to chirp scaling discussed above vary linearly with the pulse phase error coefficients,  $\Delta K$ ,  $\Delta C$ , or  $\Delta Y$ . This linear variation of processing error is much slower than, say, the increase in resolution broadening due to a pulse compression error as a function of the pulse phase error coefficient [8]. Thus, the processing error in the CS algorithm remains relatively small, even as the pulse phase error increases to values that correspond to large compression errors. For example, consider doubling the

quadratic and cubic pulse phase errors considered above, giving very large maximum pulse phase errors of  $180^\circ$  that are unlikely to occur in practice. In the case of doubling the frequency rate error, the result would be a doubling of the registration error to about 0.1 samples at the swath edge. The compression error with a fast Fourier transformed replica would still be too small to be noticed. In the case of doubling the cubic phase error, the compressed pulse phase error would approximately double to  $6^\circ$  at the swath edge, and resolution broadening due to cubic or quadratic compression errors would still be negligible. Thus, even for these very large pulse phase errors, the overall effect on processing remains the same. That is, although large enough to affect interferometry, the processing errors either can be neglected if the pulse is stable, or can be avoided if phase modulation coefficients are estimated.

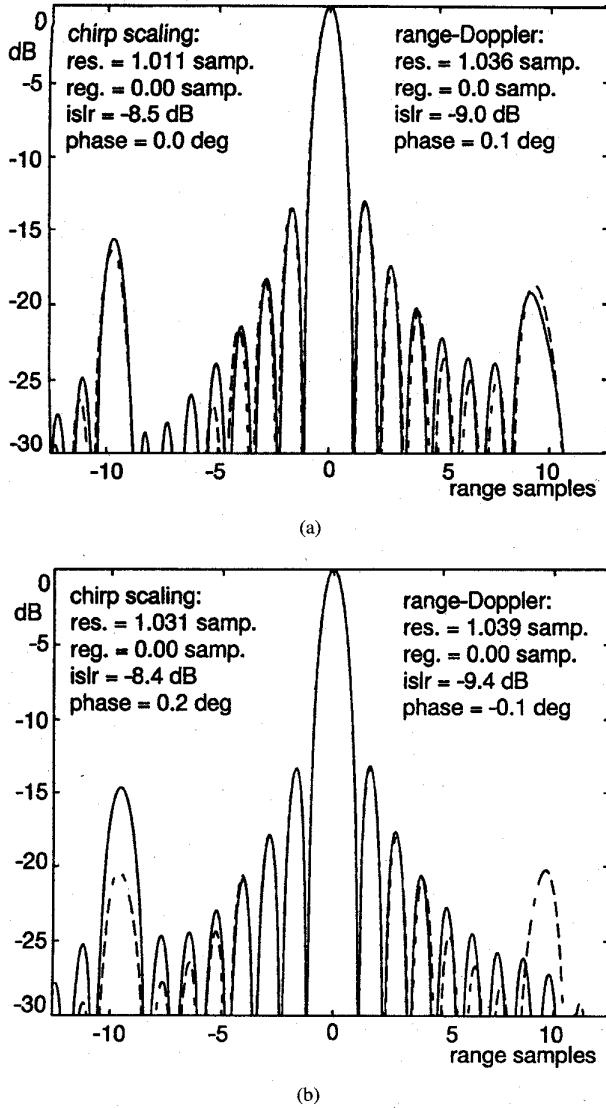


Fig. 4. Magnitude of compressed range pulses processed with the chirp scaling (solid line) and R/D (dashed line) algorithms. Transmitted pulse had a cyclic phase error: (a) no replica; (b) fast Fourier transformed replica used to obtain matched filter.

The registration and phase error described above vary linearly with  $[(\alpha - 1)\Delta\tau]$ , that is, with the amount of scaling and with distance from the reference range. These processing errors are determined at 20 km in slant range from the reference range, but the linear variation with range means the errors would remain relatively small for larger range blocks. Also, as mentioned earlier, the dependence of processing error on the amount of scaling means a dependence on the squint angle,  $\theta$ . For  $f_{\eta r} = 0$ , using small angle approximations it can be shown that  $(\alpha - 1)$  varies as  $\theta^2$ . Thus, for squint angles larger than the  $5^\circ$  considered here, the processing errors would quickly become more significant if  $f_{\eta r}$  remained at zero. Thus for higher squint, the reference azimuth frequency would have to change to remain within a certain interval of azimuth frequency from the Doppler centroid. The consequence of this

is that the processed image would not be registered at closest approach range.

Finally, other smaller processing errors from (10) and (12) vary with  $[(\alpha - 1)\Delta\tau]^2$ , and thus would increase more quickly with range and scaling. However, the errors are so small that they would remain negligible for a wide range of SAR parameters.

## VI. CONCLUSION

From the point of view of high precision SAR processing, for applications such as interferometry, the most noticeable effects of pulse phase errors on the chirp scaling algorithm are a registration and a phase error in the compressed pulse. However, these are negligible for the relatively small pulse phase errors typical in SAR systems. Larger pulse phase errors have no noticeable effect on the magnitude image, and can be neglected in interferometry if the pulse is stable. Also, the registration and phase error can be avoided in any case if phase modulation coefficients are estimated from the pulse replica.

In addition, it was found that the effect of pulse phase errors on range compression with the chirp scaling algorithm is negligible. A fast Fourier transformed pulse replica is sufficient to obtain the range matched filter, with the CS algorithm giving a slight improvement in range resolution compared to the R/D algorithm.

## APPENDIX PULSE SPECTRUM WITH ARBITRARY PHASE MODULATION ERROR

It is required to find the Fourier transform of the transmitted pulse as a function of the general small pulse phase error as in (1). For large time-bandwidth pulses such as used in SAR, the method of stationary phase provides an approximation to the Fourier transform [3]. To accommodate the general phase error in the pulse, the following approximation to the method of stationary phase has been developed. The Fourier transform of the transmitted pulse requires evaluation of the integral

$$P(f_\tau) = \int m(\tau) \exp\{-j\pi K \tau^2 - j2\pi \varepsilon(\tau) - j2\pi f_\tau \tau\} d\tau \quad (14)$$

and the equation for the stationary point is

$$K\tau + \varepsilon'(\tau) + f_\tau = 0. \quad (15)$$

To take advantage of the fact that the pulse error is small compared to the pulse phase, let  $\varepsilon(\tau)$  be represented as

$$\varepsilon(\tau) = \epsilon \rho(\tau) \quad (16)$$

where  $\epsilon$  is a small parameter.

An approximate solution for the stationary point can be found by iterating, assuming  $\epsilon$  is small, where  $\tau$  is first solved for as follows:

$$\tau \approx \frac{-f_\tau}{K} - \frac{\epsilon}{K} \rho' \left( \frac{-f_\tau}{K} - \frac{\epsilon}{K} \rho'(\tau) \right). \quad (17)$$

Then, since  $\epsilon$  is small in the argument of  $\rho'$ , the second term can be expanded in a series about  $-f_\tau/K$  to give

$$\tau \approx \frac{-f_\tau}{K} - \frac{\epsilon}{K} \rho' \left( \frac{-f_\tau}{K} \right) + \frac{\epsilon^2}{K^2} \rho'' \left( \frac{-f_\tau}{K} \right) \rho'(\tau). \quad (18)$$

Proceeding in this way, it can be seen that higher order terms in the approximation decrease as higher powers of the small parameter  $\epsilon/K$ , thus forming an asymptotic expansion for the stationary point. Keeping only the first term in  $\epsilon$  and substituting for the stationary point in the integrand gives an approximation for the Fourier transform of the pulse

$$P(f_\tau) = m\left(\frac{-f_\tau}{K}\right) \exp\left\{\frac{j\pi f_\tau^2}{K} - j2\pi\epsilon\left(\frac{-f_\tau}{K}\right)\right\} \quad (19)$$

where constants and the effect of  $\epsilon(\tau)$  on the amplitude have been neglected.

This approximation to the Fourier transform is valid for signals for which the method of stationary phase can be used, and for pulse phase errors for which the approximation to the stationary point in (18) can be made. Equation (18) requires the existence of the derivatives of  $\rho(\tau)$ , which in general is not a problem for bandlimited pulses. In particular, for polynomial pulse phase errors, the derivatives exist and (18) gives a series with terms that decrease quickly if the ratio of the pulse phase error to total pulse phase is small. For other pulse phase errors the derivatives may become large, as for the case of a cyclic pulse phase error in (13) with a large  $\omega$ . In this case, terms past a certain order in the asymptotic expansion may begin to increase, although the approximation can still be used for small pulse phase errors.

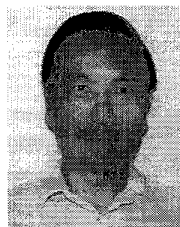
#### REFERENCES

- [1] I. G. Cumming and J. R. Bennett, "Digital processing of SEASAT SAR data," in *ICASSP'79 Proc.*, 1979, pp. 710-718.
- [2] R. K. Raney, H. Runge, R. Bamler, I. Cumming, and F. Wong, "Precision SAR processing using chirp scaling," *IEEE Trans. Geosci. Remote Sensing*, 1993, submitted for publication.
- [3] C. E. Cook and M. Bernfeld, *Radar Signals*. New York: Academic, 1967.
- [4] R. Bamler, "A comparison of range-Doppler and wavenumber domain SAR focusing algorithms," *IEEE Trans. Geosci. Remote Sensing*, vol. 30, no. 4, pp. 706-713, 1992.
- [5] G. W. Davidson, I. G. Cumming, M. R. Ito, "A chirp scaling approach for processing squint mode SAR data," *IEEE Trans. Aerosp. Electron. Syst.*, 1996, to be published.
- [6] R. Bamler, M. Eineder, H. Breit, U. Steinbrecher, and D. Just, "X-SAR data and image quality," in *IGARSS'94 Proc.*, 1994, pp. 1175-1177.
- [7] F. K. Li and R. M. Goldstein, "Studies of multibaselining spaceborne interferometric synthetic aperture radar," *IEEE Trans. Geosci. Remote Sensing*, vol. 28, no. 1, pp. 88-97, 1990.
- [8] F. H. Wong and I. G. Cumming, "Error sensitivities of a secondary range compression algorithm for processing squinted satellite SAR data," in *Proc. IGARSS'89*, 1989, pp. 2584-2587.



**Gordon W. Davidson** (S'83-M'86) received the B.Sc. degree from the University of Calgary, Canada, and the M.Eng. degree in electrical engineering from Carleton University, Ottawa, Canada, in 1984 and 1986, respectively. He received the Ph.D. degree from the University of British Columbia, Canada, in 1994, for which he investigated squint mode SAR signal properties and the chirp scaling algorithm.

From 1986 to 1988, he was with Bell Northern Research, and in 1989, he was a Research Assistant working on adaptive signal processing at Carleton University. As a student, he consulted for MacDonald Dettwiler. During 1994-1995, he was a Lecturer at the University of British Columbia. He is currently a Guest Scientist at the German Remote Sensing Data Center (DLR/DFD), Oberpfaffenhöfen, working on ScansAR and SAR interferometry.



**Frank Wong** (M'78) received the B.A.Sc. degree in electrical engineering from McGill University, Canada, in 1969, and the M.A.Sc. degree in electrical engineering from Queen's University, Canada, in 1971. He obtained the Ph.D. degree in computer science from the University of British Columbia, Canada, in 1984, specializing in image processing. He earned the Ph.D. degree while he was with MacDonald Dettwiler.

He was with Computing Devices Company in Ottawa, Canada, as a Signal Processing Engineer. In 1977 he joined MacDonald Dettwiler, where he has been doing research work in SAR processing algorithms. Currently, he is a Senior Research Engineer at MacDonald Dettwiler, and also a Sessional Lecturer at UBC, teaching a course in remote sensing. In 1994, he was a UBC Visiting Industrial Scientist in the Radar Research Group, and his visit was sponsored by MDA and the BC Advanced Systems Institute.



**Ian Cumming** (S'63-M'66) received the B.Sc. degree in engineering physics at the University of Toronto, Toronto, Canada, in 1961, and the Ph.D. degree in computing and automation from Imperial College, University of London, U.K., in 1968.

Following work in steel mill automation and sonar signal processing, he joined MacDonald Dettwiler and Associates in 1977. Since that time, he has developed synthetic aperture radar signal processing algorithms, and has worked on systems for processing polarimetric and interferometric radar data, and for the compression of radar data. In 1993, he joined the Department of Electrical Engineering, University of British Columbia, Canada, where he holds the MacDonald Dettwiler/NSERC Industrial Research Chair in Radar Remote Sensing. The associated laboratory supports a research staff of 10 engineers and students, working in the fields of SAR processing, SAR data encoding, satellite SAR two-pass interferometry, airborne along-track interferometry, airborne polarimetric radar classification, and SAR Doppler estimation.